Neural Map Prior for Autonomous Driving

Xuan Xiong[1] Yicheng Liu[1] Tianyuan Yuan[2] Yue Wang[3] Yilun Wang[2] Hang Zhao[2,1*]

[1]Shanghai Qi Zhi Institute [2]IIIS, Tsinghua University [3]MIT

Abstract

High-definition (HD) semantic maps are crucial for autonomous vehicles navigating urban environments. Traditional offline HD maps, created through labor-intensive manual annotation processes, are both costly and incapable of accommodating timely updates. Recently, researchers have proposed inferring local maps based on online sensor observations; however, this approach is constrained by the sensor perception range and is susceptible to occlusions. In this work, we propose ***Neural Map Prior (NMP)****, a neural representation of global maps that facilitates automatic global map updates and improves local map inference performance. To incorporate the strong map prior into local map inference, we employ cross-attention that dynamically captures correlations between current features and prior features. For updating the global neural map prior, we use a learning-based fusion module to guide the network in fusing features from previous traversals. This design allows the network to capture a global neural map prior during sequential online map predictions. Experimental results on the nuScenes dataset demonstrate that our framework is highly compatible with various map segmentation and detection architectures and considerably strengthens map prediction performance, even under adverse weather conditions and across longer horizons. To the best of our knowledge, this represents the first learning-based system for constructing a global map prior.*

1. Introduction

Autonomous vehicles require high-definition (HD) semantic maps to accurately predict the future trajectories of other agents and safely navigate urban streets. However, most autonomous vehicles depend on labor-intensive and costly pre-annotated offline HD maps, which are constructed through a complex pipeline involving multi-trip LiDAR scanning with survey vehicles, global point cloud alignment, and manual map element annotation. Despite their high precision, the scalability of these offline mapping solutions is limited, and they do not support timely updates when road conditions change. Consequently, autonomous vehicles may rely on out-of-date maps, negatively impacting driving safety. Recent research has explored alternative methods for learning HD semantic maps using onboard sensor observations, such as camera images and LiDAR point clouds [11, 13, 15]. These methods typically use deep learning techniques to infer map elements in real-time, addressing the map update issue associated with offline maps. However, the quality of the inferred maps is generally infe-

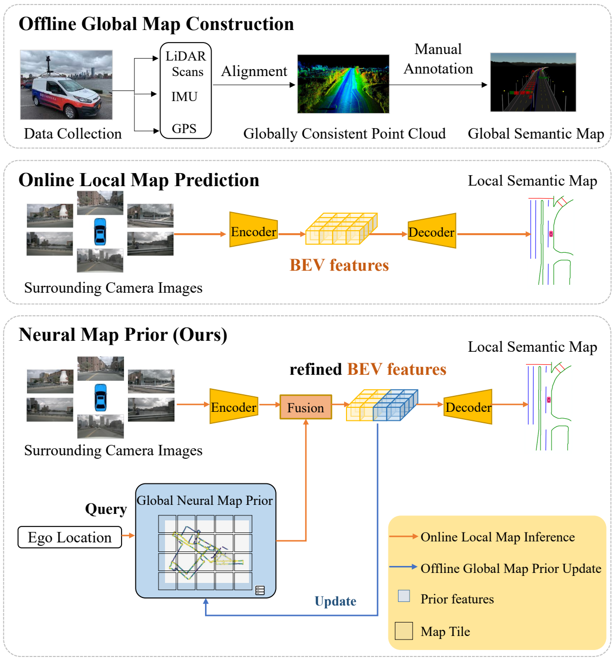

Figure 1. **Comparison of semantic map construction methods.** Traditional offline semantic mapping pipelines (the first row) involve a complex manual annotation pipeline and do not support timely map updates. Online HD semantic map learning methods (the second row) rely entirely on onboard sensor observations and are susceptible to occlusions. We propose the Neural Map Prior (NMP, the third row), an innovative neural representation of global maps designed to aid onboard map prediction. NMP is incrementally updated as it continuously integrates new observations from a fleet of autonomous vehicles.

[*]Corresponding at: hangzhao@mail.tsinghua.edu.cn.

rior to pre-constructed global maps and may further deteriorate under adverse weather conditions and occluded scenarios. The comparison of different semantic map construction methods is illustrated in Figure 1.

In this work, we propose Neural Map Prior (NMP), a novel hybrid mapping solution that combines the best of both worlds. NMP leverages neural representations to build and update a global map prior, thereby improving map inference performance for autonomous cars. The NMP process consists of two primary steps: **global map prior update** and **local map inference**. The global map prior is a sparsely tiled neural representation, with each tile corresponding to a specific real-world location. It is automatically developed by aggregating data from a fleet of self-driving cars. Onboard sensor data and the global map prior are then integrated into the local map inference process, which subsequently refines the map prior. These procedures are interconnected in a feedback loop that grows stronger as more data is collected from the vast number of vehicles navigating the roads daily. One example is shown in Figure 2.

Technically, the global neural map prior is defined as **sparse map tiles** initialized from an empty state. For each online observation from an autonomous vehicle, a neural network encoder first extracts local Birds-Eye View (BEV) features. These features are then refined using the corresponding BEV prior feature derived from the global NMP's map tile. The improved BEV features enable us to infer the local semantic map and update the global NMP. As the vehicles traverse through the various scenes, the local map inference phase and the global map prior update step mutually reinforce each other, improving the quality of the predicted local semantic map and maintaining a more complete and up-to-date global NMP.

We demonstrate that NMP can be readily applied to various state-of-the-art HD semantic map learning methods to enhance accuracy. Experiments on the public nuScenes dataset reveal that by integrating NMP with cutting-edge map learning techniques, our pipeline improves performance by **+4.32** mIoU for HDMapNet, **+5.02** mIoU for LSS, **+5.50** mIoU for BEVFormer, and **+3.90** mAP for VectorMapNet.

To summarize, our contributions are as follows:

1. We propose a novel mapping paradigm named Neural Map Prior that combines offline global map maintenance and online local map inference, while local inference demands similar computational and memory resources as previous single-frame systems.
2. We propose simple and efficient current-to-prior attention and GRU modules adaptable to mainstream HD semantic map learning methods and boost their map prediction results.
3. We evaluate our method on the nuScenes dataset across different map elements and four map segmentation/detection architectures and demonstrate significant and consistent improvements. Moreover, our findings show notable progress in challenging situations involving adverse weather conditions and extended perception ranges.

2. Related Works

LiDAR SLAM-Based Mapping. Autonomous driving system requires an understanding of road map elements, including lanes, pedestrian crossing, and traffic signs, to navigate the world. Such map elements are typically provided by pre-annotated High-Definition (HD) semantic maps in existing pipelines [27]. Most current HD semantic maps are manually or semi-automatically annotated on LiDAR point clouds of the environment, merged from LiDAR scans collected from survey vehicles equipped with high-end GPS and IMU. SLAM algorithms are the most commonly used algorithms to fuse LiDAR scans into a highly accurate and consistent point cloud. First, to match LiDAR data at two nearby timestamps, pairwise alignment algorithms such as ICP [1], NDT [2], and their variants [30] are employed, using either semantic [40] or geometry information [24]. Second, accurately estimating the poses of the ego vehicles is critical for building a globally consistent map and is formulated as either a non-linear least-square problem [10] or a factor graph [7]. Yang et al. [36] presented a method for reconstructing city-scale maps based on pose graph optimization under the constraint of pairwise alignment factors. To reduce the cost of manual annotation of semantic maps, Jian et al. [9] proposed several machine-learning techniques for extracting static elements from fused LiDAR point clouds and cameras. However, maintaining an HD semantic map remains a laborious and costly process due to the requirement for high precision and timely updates. In this paper, we propose using neural map priors as a novel mapping paradigm to replace human-curated HD maps, supporting timely updates to the global map prior and enhancing local map learning, potentially making it a more scalable solution for autonomous driving.

Semantic Map Learning. Semantic map learning constitutes a fundamental challenge in real-world map construction and has been formulated as a semantic segmentation problem in [18]. Various approaches have been employed to address this issue, including aerial images in [19], LiDAR point clouds in [35], and HD panoramas in [32]. To enhance fine-grained segmentation performance, crowdsourcing tags have been proposed in [33]. Recent studies have concentrated on deciphering BEV semantics from onboard camera images [17, 37] and videos [4]. Relying solely on onboard sensors for model input poses a challenge, as the inputs and target map belong to different co-

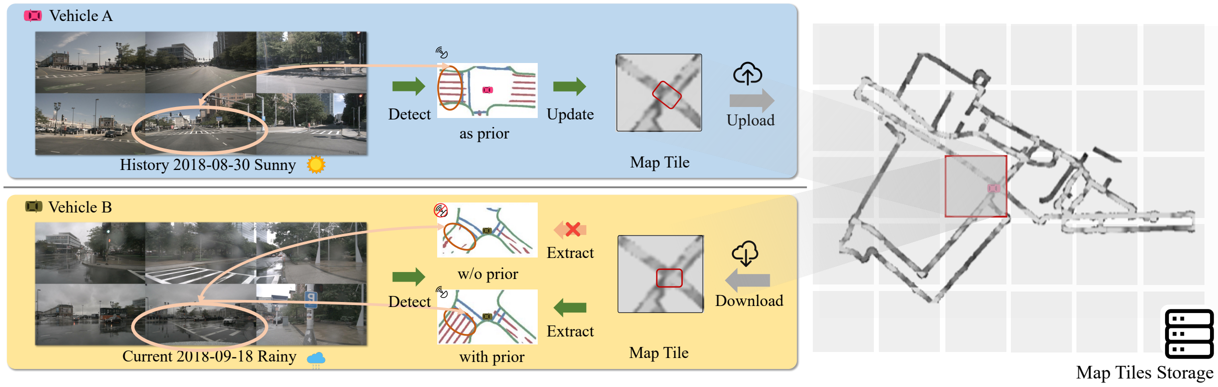

(a) The map prior update from sunny days help with rainy days.

(b) Global Neural Map Prior

Figure 2. **Demonstration of NMP for autonomous driving in adverse weather conditions.** Ground reflections during rainy days make online HD map predictions harder, posing safety issues for an autonomous driving system. NMP helps to make better predictions, as it incorporates prior information from other vehicles that have passed through the same area on sunny days.

ordinate systems. Cross-view learning methodologies, such as those found in [5,11,21,23,26,28,34,41], exploit scene geometric structures to bridge the gap between sensor inputs and BEV representations. Our proposed method capitalizes on the inherent spatial properties of BEV features as a neural map prior, making it compatible with a majority of BEV semantic map learning techniques. Consequently, this approach holds the potential to enhance online map prediction capabilities.

Neural Representations. Recently, advances have been made in neural representations [8, 14, 20, 22, 29, 38]. NeuralRecon [31] presents an approach for implicit neural 3D reconstruction that integrates reconstruction and fusion processes. Unlike traditional methods that first estimate depths and subsequently perform fusion offline. Similarly, our work learns neural representation by employing the encoded image features to predict the map prior through a neural network.

3. Neural Map Prior

The aim of this work is to improve local map estimation performance by leveraging a global neural map prior. To achieve this, we propose a pipeline, depicted in Figure 3, which is specifically designed to concurrently train both the global map prior update and local map learning while integrating a fusion component. Moreover, we address the memory-intensive challenge associated with storing features of urban streets by introducing a sparse tile format for the global neural map prior, details provided in Section 4.8.

Problem Setup. Our model operates on typical autonomous driving systems equipped with an array of onboard sensors, such as surround-view cameras and GPS/IMU, for precise localization. We assume a single-frame setting, similar to [11], which adopts a BEV encoder-decoder model for inferring local semantic maps. The BEV encoder is denoted as F_{enc}, and the decoder is denoted as F_{dec}. Additionally, we create and maintain a global neural map prior $p^g \in \mathbb{R}^{H_G \times W_G \times C}$, where H_G and W_G represent the height and width of the city, respectively. Each observation consists of input from the surrounding cameras $\mathbf{I}$ and the ego vehicle's position in the global coordinate system $\mathbf{G}_{\text{ego}} \in \mathbb{R}^{4\times 4}$. We can transform the local coordinate of each pixel of the BEV, denoted as $l_{\text{ego}} \in \mathbb{R}^{H \times W \times 2}$ (where H and W denote the size of the BEV features), to a fixed global coordinate system using $\mathbf{G}_{\text{ego}}$. This transformation results in $p_{\text{ego}} \in \mathbb{R}^{H \times W \times 2}$. Initially, we acquire the online BEV features $o = F_{enc}(\mathbf{I}) \in \mathbb{R}^{H \times W \times C}$, where C represents the network's hidden embedding size. We then query the global prior p^g using the ego position p_{ego} to obtain the local prior BEV features $p^l_{t-1} \in \mathbb{R}^{H \times W \times C}$. A fusion function is subsequently applied to the online BEV features, and the local prior BEV features to yield refined BEV features:

$$f_{\text{refine}} = F_{\text{fuse}}(o, p^l_{t-1}), f_{\text{refine}} \in \mathbb{R}^{H \times W \times C}. \tag{1}$$

Finally, the refined BEV features are decoded into the final map outputs by the decoder F_{dec}. Simultaneously, the global map prior p^g is updated using f_{refine}. The global neural network prior acts as an external memory, capable of incrementally integrating new information and simultaneously offering knowledge output. This dual functionality ultimately leads to improved local map estimation performance.

3.1. Local Map Learning

In order to accommodate the dynamic nature of road networks in the real world, advanced online map learning algorithms have recently been developed. These methods generate semantic map predictions based solely on data collected by onboard sensors. In contrast to earlier approaches, our proposed method incorporates neural priors

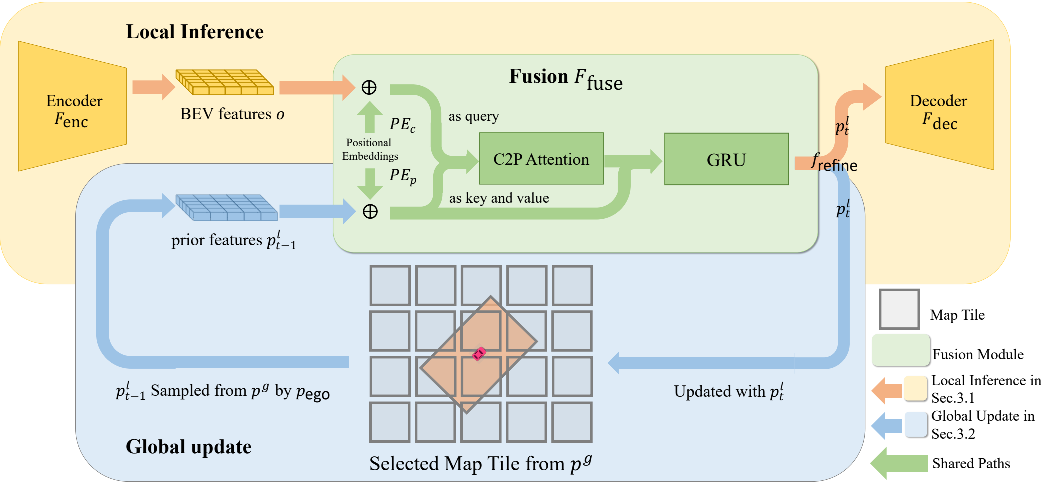

Figure 3. **The model architecture of NMP.** The top yellow box illustrates the online HD map learning process, which takes images as input and processes them through a BEV encoder and decoder to generate map segmentation results. Within the green box, customized fusion modules—comprising C2P attention and GRU—are designed to effectively integrate prior map features between the encoder and decoder, subsequently decoded to produce the final map predictions. In the bottom blue box, the model queries map tiles that overlap with the current BEV feature from storage. After the update, the neural map is returned to the previously extracted map tiles.

to bolster accuracy. As road structures on maps are subject to change, it is imperative that recent observations take precedence over older ones. To emphasize the importance of current features, we introduce an asymmetric fusion strategy that combines current-to-prior attention and gated recurrent units.

Current-to-Prior Cross Attention. We introduce the current-to-prior cross-attention mechanism, which employs a standard cross-attention approach [16] to operate between current and prior BEV features. Concretely, We divide each feature into patches and add them with a set of learnable positional embeddings, which will be described subsequently. Following this, we transform each patch into a token using a fully connected layer. Current feature tokens serve as queries, while prior feature tokens act as keys and values. A standard cross-attention is then applied, succeeded by a fully connected layer. Ultimately, we assemble the output queries to derive the refined BEV features, which maintain the same dimensions as the input current features. The resulting refined BEV features are expected to exhibit superior quality compared to both prior and current features.

Positional Embedding. It has been observed that the accuracy of predicted maps declines as the distance from the ego vehicle increases. To address this issue, we propose the integration of position embeddings, a set of grid-shaped learnable parameters, into the fusion module. The aim is to augment the spatial awareness of the fusion module regarding the feature positions, empowering it to learn to trust the current features closer to the ego vehicle and rely more on the prior features for distant locations. Specifically, two position embeddings are introduced: $PE_p \in \mathbb{R}^{H\times W\times C}$ for the prior features and $PE_c \in \mathbb{R}^{H\times W\times C}$ for the current features, respectively, before the fusion module F_{fuse}. Here, H and W represent the height and width of the BEV features. These embeddings provide spatial awareness to the fusion module, effectively allowing it to assimilate information from varying feature distances and locations.

3.2. Global Map Prior Update

To update the global map prior with the refined features generated by the C2P attention module, an auxiliary module is introduced, devised to attain a balanced ratio between the current and prior features. This process is illustrated in Figure 3. Intuitively, the module regulates the updating rate of the global map prior. A high update rate may lead to corruption of the global map prior due to suboptimal local observations, while a low update rate may result in the global map prior's inability to promptly capture changes in road conditions. Therefore, we introduce a 2D convolutional variant of the Gated Recurrent Unit [6] module into NMP, serving to balance the updating and forgetting ratio. The refined features generated by the C2P attention module are denoted as $o^{'}$. Local map prior features p_{t-1}^l, updated at $t-1$, are extracted from the global neural map prior p_{t-1}^g. The GRU fuses $o^{'}$ with the local prior features p_{t-1}^l to obtain the new prior features p_t^l at time t. These features are then passed through the decoder to predict the local semantic map. Subsequently, the global neural map prior p_t^g is updated at the corresponding location by directly replacing them with p_t^l. Formally, let z_t represent the update gate, r_t the reset gate,

σ the sigmoid function, and w_* the weight for 2D convolution. The operator $\odot$ denotes the Hadamard product. The GRU fuses $o^{'}$ with the prior feature p^l_{t-1} through the following operations:

$$
\begin{aligned}
z_t &= \sigma(\text{Conv2D}([p^l_{t-1}, o^{'}], w_z)) \\
r_t &= \sigma(\text{Conv2D}([p^l_{t-1}, o^{'}], w_r)) \\
\tilde{p^l_t} &= \tanh(\text{Conv2D}([r_t \odot p^l_{t-1}, o^{'}], w_h)) \\
p^l_t &= (1 - z_t) \odot p^l_{t-1} + z_t \odot \tilde{p^l_t}
\end{aligned}
\tag{2}
$$

The update gate z_t and reset gate r_t in the GRU are instrumental in determining the fusion of information from the previous traversal (*i.e.*, prior feature p^l_{t-1}) with the current BEV feature $o^{'}$. Furthermore, they govern the incorporation of information from the current BEV feature $o^{'}$ into the global map prior feature p^l_t. The GRU functions as a selective attention mechanism in a data-driven approach, supplanting certain hand-crafted linear updating rules. This data-driven approach enables the model to adapt to various road conditions and mapping scenarios more effectively.

4. Experiments

Datasets. We validate our NMP on the nuScenes dataset [3], a large-scale autonomous driving benchmark comprising multiple traversals with precise localization and annotated HD map semantic labels. The dataset comprises 700 scenes in the *train* set, 150 in the *val* set, and 150 in the *test* set. Data were collected using a 32-beam LiDAR operating at 20 Hz and six cameras providing a 360-degree field of view at 12 Hz. Annotations for keyframes are supplied at 2 Hz. Each scene lasts 20 seconds, resulting in 28,130 and 6,019 frames for the training and validation sets, respectively.

Metric. The HD semantic learning quality is evaluated using Mean Intersection over Union (mIoU) and Average Precision (AP) presented in HDMapNet [11]. Following the methodology outlined in HDMapNet, we evaluate three static map elements: road boundary, lane divider, and pedestrian crossing on the nuScenes dataset.

4.1. Implementation Details

Base models. We incorporate our NMP paradigm into four recently proposed camera-based map semantic segmentation/detection methods, which serve as our baselines: HDMapNet [11], LSS [23], BEVFormer [12], and VectorMapNet [15]. These methods employ four different 2D-3D feature-lifting strategies: MLP-based unprojection by HDMapNet, depth-based unprojection by LSS, geometry-aware transformer-like models by BEVFormer, and homography-based unprojection by VectorMapNet. Unless otherwise specified, our experiments are conducted on the BEVFormer model, the version without the temporal aspect, which has strong BEV feature extraction capability and achieves state-of-the-art map semantic segmentation results. For the comparisons presented in Table 4 and Table 7, we utilize only the GRU fusion module.

Table 1. **Quantitative analysis of map segmentation.**The performance of online map segmentation methods and their NMP versions on the nuScenes validation set. By adding prior knowledge, NMP consistently improves these methods.

Model	mIoU			
	Divider	Crossing	Boundary	All
HDMapNet	41.04	16.23	40.93	32.73
HDMapNet + NMP	**44.15**	**20.95**	**46.07**	**37.05**
△ mIoU	+3.11	+4.72	+5.14	+4.32
LSS	45.19	26.90	47.27	39.78
LSS + NMP	**50.20**	**30.66**	**53.56**	**44.80**
△ mIoU	+5.01	+3.76	+6.29	+5.02
BEVFormer	49.51	28.85	50.67	43.01
BEVFormer + NMP	**55.01**	**34.09**	**56.52**	**48.54**
△ mIoU	+5.50	+5.24	+5.95	+5.53

Table 2. **Quantitative analysis of map detection.**The performance of map detection method and its NMP version on the nuScenes validation set. Results show that by adding prior knowledge, the NMP enhances the quality of VectorMapNet.

Model	Average Precision			
	$AP_{Divider}$	$AP_{Crossing}$	$AP_{Boundary}$	mAP
VectorMapNet	47.3	36.1	39.3	40.9
VectorMapNet + NMP	**49.6**	**42.9**	**41.9**	**44.8**
△ AP	+2.3	+6.8	+2.6	+3.9

C2P Attention. For all linear layers within the current-to-prior attention module, we set the dimension of the features to 256. For patching, we use a patch size of 10 × 10, corresponding to a 3m × 3m area in BEV. This setting preserves local spatial information while conserving parameters. The MLP layer following the cross-attention module is also a fully connected layer with 256 filters.

Global Map Resolution. We use a default map resolution of 0.3m for the rasterized neural map priors for all experiments and conduct an ablation study on the resolution in Table 7.

4.2. Neural Map Prior Helps Online Map Inference

In this section, we show that the efficacy of NMP is agnostic to model architectures and evaluation metrics. To illustrate this, we add NMP to four base models previously mentioned: HDMapNet, LSS, BEVFormer, and VectorMapNet. We adhere to the same hyperparameter settings as in the original designs. During training, we freeze all the modules before the BEV features and train only the C2P Attention module, the GRU, the Local PE, and the decoder.

Table 3. **Comparison of model performance at different BEV ranges.** As the perception range increases, it is difficult for the online method to achieve good results; NMP significantly improves the results.

BEV Range	+ NMP	mIoU			
		Divider	Crossing	Boundary	All
$60m \times 30m$	X	49.51	28.85	50.67	43.01
	✓	**55.01**	**34.09**	**56.52**	**48.54**
$\triangle$ mIoU		+5.50	+5.24	+5.95	+5.53
$100m \times 100m$	X	43.41	29.07	56.57	43.01
	✓	**49.51**	**32.67**	**59.94**	**47.37**
$\triangle$ mIoU		+6.10	+3.60	+3.60	+4.36
$160m \times 100m$	X	41.21	26.42	51.74	39.79
	✓	**46.85**	**29.25**	**57.22**	**44.44**
$\triangle$ mIoU		+5.64	+2.83	+5.48	+4.65

Table 4. **Comparison of intra-trip fusion and inter-trip fusion.**

Intra or Inter Trips	mIoU			
	Divider	Crossing	Boundary	All
Baseline	49.51	28.85	50.67	43.01
Intra-trip fusion	51.87	30.34	53.74	45.31(+2.30)
Inter-trip fusion	**53.41**	**31.92**	**55.15**	**46.82(+3.81)**

Table 5. **Performance in adverse weather conditions.**

Weather	+ NMP	mIoU			
		Divider	Crossing	Boundary	All
Rain	X	50.25	26.90	44.54	40.56
	✓	**54.64**	**30.62**	**54.19**	**46.48**
$\triangle$ mIoU		+4.39	+3.72	+9.65	+5.92
Night	X	51.02	21.17	48.99	40.39
	✓	**54.66**	**33.78**	**55.92**	**48.12**
$\triangle$ mIoU		+3.64	+12.61	+6.93	+7.73
NightRain	X	55.76	00.00	47.60	34.45
	✓	**61.22**	00.00	**50.84**	**37.35**
$\triangle$ mIoU		+5.46	+00.00	+3.24	+2.90
Normal	X	49.27	29.49	52.11	43.62
	✓	**53.46**	**35.27**	**57.75**	**48.82**
$\triangle$ mIoU		+4.19	+5.78	+5.64	+5.20

For testing, all samples are sorted chronologically. As evidenced in Table 1 and Table 2, NMP consistently improves map segmentation and detection performance over baseline counterparts. Qualitative results can be found in Figure 4. They indicate that the NMP is generic and could potentially be applied to other map learning frameworks as well.

4.3. Neural Map Prior Helps to See Further

One traditional role of maps is to provide information about roads beyond the horizon, which is essential for downstream navigation and planning and aids in making informed decisions. Our proposed neural map prior serves this vital function by allowing onboard map inference to extend its range. As shown in Table 3, our neural map prior consistently improves the segmentation results of the map for the baseline methods for BEV range spanning $60m \times 30m$, $100m \times 100m$, and $160m \times 100m$. Camera-based map segmentation and detection are typically considered challenging in the most distant regions of the map from the ego vehicle, as these areas only occupy a few pixels in the image. Therefore, incorporating the prior history of the scenes is crucial for enhancing map segmentation and detection performance.

4.4. Inter-trip Fusion is better than Intra-trip Fusion

In Table 4, we analyze the relative importance of intra-trip information versus inter-trip information. Specifically, intra-trip information refers to the scenario where the available map prior is constrained to a single traversal, whereas the inter-trip information model uses map priors generated from any traversals at the same location. The results suggest that incorporating multi-traversal prior information is more critical for map construction, as the performance of the intra-trip model is inferior compared to the inter-trip one.

4.5. Neural Map Prior is more helpful under Adverse Weather Conditions

Autonomous vehicles face inevitable challenges when driving in adverse weather conditions, such as rain or night driving, which can make it challenging for the vehicle to accurately identify road information. However, the Neural Map Prior obtained under better weather and lighting conditions, can provide more reliable information for the vehicle to perceive road information accurately. As shown in Table 5 that using the neural map prior in adverse weather conditions, such as rain and night driving, leads to more substantial improvements than in normal weather conditions, indicating that our model effectively extracts the necessary information from the NMP to handle adverse weather scenarios. However, the improvement was less significant during night-rain conditions due to the limited available map prior information and a smaller sample size.

4.6. Ablation Studies on Fusion Components

GRU, C2P Attention and Local Position Embedding. In this section, we evaluate the effectiveness of the components proposed in Section 3. For comparison purposes, we introduce a simple fusion baseline, referred to as Moving Average (MA). MA replaces C2P Attention and GRU with a moving average fusion function. The update rule can be expressed as:

$$p_t^l = \alpha o + (1 - \alpha) o_{t-1}^l, \tag{3}$$

Table 6. **Ablation on the fusion components.** MA stands for Moving Average. Local PE stands for the positional embedding proposed in § 3.1. CA stands for the C2P Attention proposed in § 3.1 and GRU stands for gated recurrent units proposed in § 3.2.

Component					mIoU			
Name	MA	GRU	Local PE	CA	Divider	Crossing	Boundary	All
A					49.51	28.85	50.67	43.01
B	✓				52.19(+2.68)	33.70(+4.85)	55.34(+4.67)	47.07(+4.06)
C		✓			53.22(+3.71)	31.46(+2.61)	55.93(+5.26)	46.87(+3.86)
D				✓	53.25(+3.74)	33.13(+4.28)	55.15(+4.48)	47.17(+4.16)
E		✓	✓		52.96(+3.45)	**34.13(+5.28)**	56.14(+5.47)	47.74(+4.73)
F		✓		✓	**55.05(+3.74)**	31.37(+2.52)	56.19(+5.52)	47.53(+4.52)
G		✓	✓	✓	55.01(+5.50)	34.09(+5.24)	**56.52(+5.85)**	**48.54(+5.53)**

Table 7. **Ablation on the resolution for Map**: 0.3m × 0.3m is the good design choice that balances storage size and accuracy.

NMP Grid Resolution	mIoU			
	Divider	Crossing	Boundary	All
Baseline	49.51	28.85	50.67	43.01
0.3m × 0.3m	**53.22**	31.46	**55.93**	**46.87(+3.86)**
0.6m × 0.6m	52.42	**31.63**	54.74	46.26(+3.25)
1.2m × 1.2m	51.36	30.24	52.78	44.79(+1.78)

Table 8. **Performance on Boston split.** The original split contains unbalanced historical trips for the training and validation sets; Boston split is more balanced.

Data Split	+ NMP	mIoU			
		Divider	Crossing	Boundary	All
Boston Split	X	26.35	15.32	25.06	22.24
	✓	**33.04**	**21.72**	**32.63**	**29.13**
△ mIoU		+6.69	+6.40	+7.57	+6.89
Original Split	X	49.51	28.85	50.67	43.01
	✓	**55.01**	**34.09**	**56.52**	**48.54**
△ mIoU		+5.50	+5.24	+5.95	+5.53

where α denotes a manually searched ratio, and other notations are defined in Section 3.2. Although both GRU and MA exhibit similar performance enhancements as updating modules, GRU is favored due to the elimination of manual parameter searches required in MA.

Table 6 illustrates that C2P Attention, Local PE, and GRU are all essential in enhancing online map prediction performance. Both GRU and CA act as effective feature fusion modules, leading to notable enhancements. CA slightly outperforms GRU, indicating that the transformer holds a minor advantage in fusing prior feature contexts.

Comparing C to E and F to G, Local PE increases the IoU of the crossing by 2.67 and 2.72, respectively, suggesting that Local PE improved feature fusion, particularly in the challenging pedestrian crossing category. Local PE enables the model to extract additional information from the map prior, complementing current observations. In comparisons between C and F and E and G, CA boosts the IoU of the lane divider by 1.83 and 2.05, respectively, highlighting its capability to handle lane structures. The attention mechanism extracts relevant features from the spatial context, leading to a more accurate understanding of divider and boundary structures. The ablation study confirms the effectiveness of all three proposed components for feature fusion and updating.

Map Resolution. We investigate the impact of different resolutions of global neural priors on the effectiveness of online map learning in Table 7. High resolutions are preferred to preserve details on the map. However, there is a trade-off between storage and resolution. Our experiments achieved good performance with an appropriate resolution of 0.3m.

4.7. Generalization

The improvement of neural network priors for online map inference is attributed to the generation of neural priors from other trips, which provide closer observations and complementary perspectives to enable the current observation to "see" further or bypass obstacles. However, data devoid of past trip observations cannot benefit from the improvement offered by neural network priors. The nuScenes dataset was not originally designed to evaluate the efficacy of utilizing historical traversals. Some samples in the datasets lack past traversals. Thus, we follow the approach presented in Hindsight [39] and re-split the datasets ensuring each training and test sample strives to possess one past trip, with geographically disjoint sequences in the training and test sets. Our split differs from Hindsight in that our proposed method for identifying historical trips is more precise, as we accurately calculate the overlap between historical and current frames instead of merely comparing the overall proximity of the two traversals. This results in 7354/6504 training/test samples in the nuScenes dataset. As demonstrated in Table 8, we observe that the baseline result of the Boston split is lower than the original split. The problem of poor generalization of map learning has also been noted in the UniFormer [25]. However, the improvement

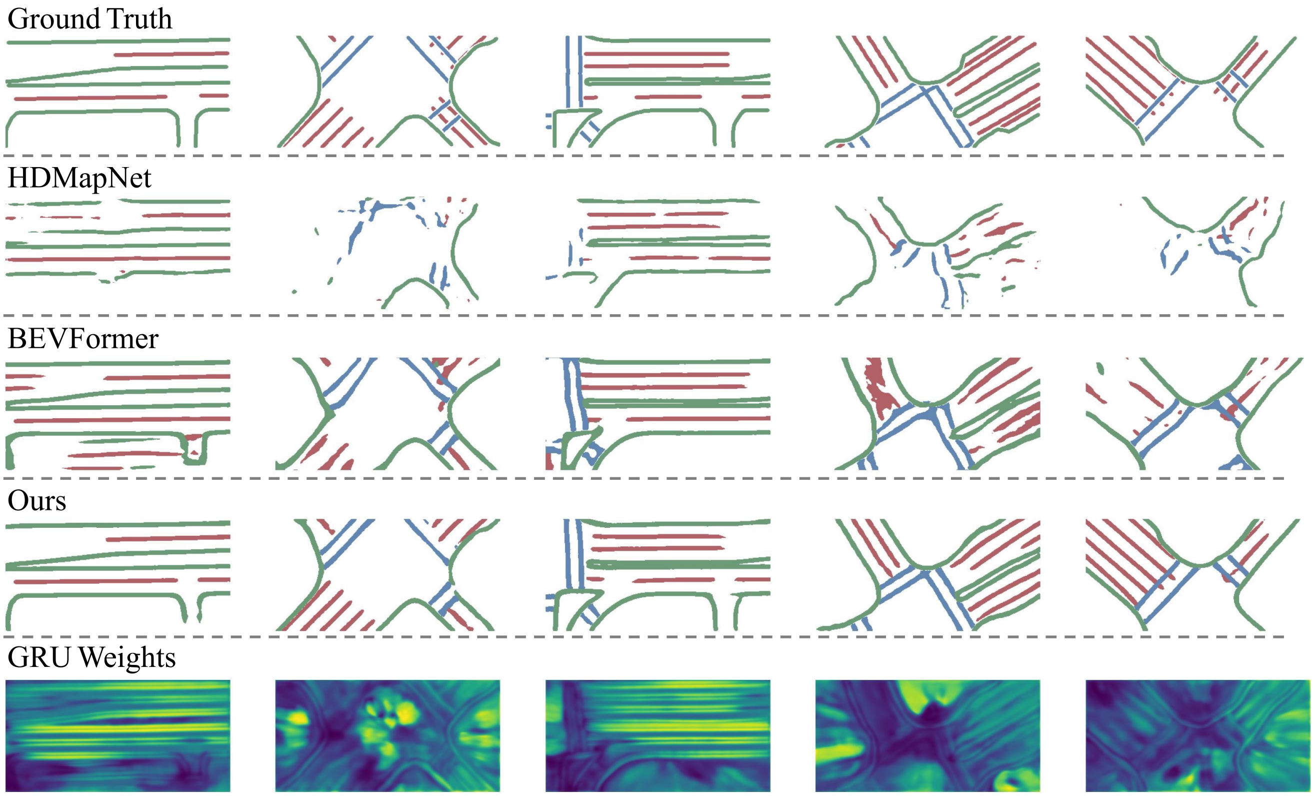

Figure 4. **Qualitative results.** From the first to the fifth row: Ground truth, HDMapNet, BEVFormer and BEVFormer with Neural Map Prior and GRU weights. We also visualize z_t, the attention map of the last step of the GRU fusion process. The model learns to selectively combine current and prior map features: specifically, when the prediction quality of the current frame is good, the network tends to learn a larger z_t, assigning more weight to the current feature; when the prediction quality of the current frame is poor, usually at intersections or locations farther away from the ego-vehicle, the network tends to learn a smaller z_t for the prior feature.

observed in the Boston split with the neural map prior is greater than that of the original split, suggesting that the poor generalization problem in map learning can be alleviated to a certain extent by our method.

4.8. Map Tiles

We use map tile as the storage format for our global neural map prior. In urban environments, buildings generally occupy a substantial portion of the area, whereas road-related regions account for a smaller part. To prevent the map's storage size from expanding excessively in proportion to the physical scale of the city, we designed a storage structure that divides the city into sparse pieces indexed by their physical coordinates. For example, in the nuScenes dataset, the Boston map covers an urban area with 2 km in height and 1.5 km in width. If we choose a feature dimension of 256 channels for the neural map prior, a 0.3m resolution for the tiles, and each tile has a size of 69m × 49m, it would take 38 GB to store the whole map features. Practically, not all map tiles overlap with roads. By removing those offroad map tiles, the map size reduces to 11 GB. Furthermore, each vehicle does not need to store the entire city map; instead, it can download map tiles on demand.

The trained model remains fixed, but these map tiles are updated, integrated, and uploaded to the cloud asynchronously. As more trip data is collected over time, the map prior becomes broader and of better quality.

5. Conclusion

In this paper, we present a novel system, Neural Map Prior, designed to aid online HD semantic map learning. The core concept involves jointly performing global map prior updates and local map inference for each frame incrementally, utilizing C2P-Attention and GRU. We propose sparse map tiles as a memory-efficient approach for maintaining map priors, enabling low-latency on-board computing. Comprehensive analysis of the large-scale nuScenes dataset demonstrates that Neural Map Prior improves map prediction performance in adverse weather and extends the prediction horizon. We believe that Neural Map Prior opens up new possibilities for learning-based multi-view and self-driving perception and recognition systems by facilitating training with downstream tasks.

References

[1] Paul J Besl and Neil D McKay. Method for registration of 3-d shapes. In *Sensor fusion IV: control paradigms and data structures*, volume 1611, pages 586–606. Spie, 1992. 2

[2] Peter Biber and Wolfgang Straßer. The normal distributions transform: A new approach to laser scan matching. In *Proceedings 2003 IEEE/RSJ International Conference on Intelligent Robots and Systems (IROS 2003)(Cat. No. 03CH37453)*, volume 3, pages 2743–2748. IEEE, 2003. 2

[3] Holger Caesar, Varun Bankiti, Alex H Lang, Sourabh Vora, Venice Erin Liong, Qiang Xu, Anush Krishnan, Yu Pan, Giancarlo Baldan, and Oscar Beijbom. nuscenes: A multimodal dataset for autonomous driving. In *Proceedings of the IEEE/CVF conference on computer vision and pattern recognition*, pages 11621–11631, 2020. 5

[4] Yigit Baran Can, Alexander Liniger, Ozan Unal, Danda Paudel, and Luc Van Gool. Understanding bird's-eye view semantic hd-maps using an onboard monocular camera. *arXiv preprint arXiv:2012.03040*, 2020. 2

[5] Xuanyao Chen, Tianyuan Zhang, Yue Wang, Yilun Wang, and Hang Zhao. Futr3d: A unified sensor fusion framework for 3d detection. *arXiv preprint arXiv:2203.10642*, 2022. 3

[6] Junyoung Chung, Caglar Gulcehre, KyungHyun Cho, and Yoshua Bengio. Empirical evaluation of gated recurrent neural networks on sequence modeling. *arXiv preprint arXiv:1412.3555*, 2014. 4

[7] Frank Dellaert. Factor graphs and gtsam: A hands-on introduction. Technical report, Georgia Institute of Technology, 2012. 2

[8] Chiyu Jiang, Avneesh Sud, Ameesh Makadia, Jingwei Huang, Matthias Nießner, and Thomas Funkhouser. Local implicit grid representations for 3d scenes. In *CVPR*, 2020. 3

[9] Jialin Jiao. Machine learning assisted high-definition map creation. In *2018 IEEE 42nd Annual Computer Software and Applications Conference (COMPSAC)*, volume 1, pages 367–373. IEEE, 2018. 2

[10] Charles L Lawson and Richard J Hanson. *Solving least squares problems*. SIAM, 1995. 2

[11] Qi Li, Yue Wang, Yilun Wang, and Hang Zhao. Hdmapnet: A local semantic map learning and evaluation framework. *arXiv preprint arXiv:2107.06307*, 2021. 1, 3, 5

[12] Zhiqi Li, Wenhai Wang, Hongyang Li, Enze Xie, Chonghao Sima, Tong Lu, Qiao Yu, and Jifeng Dai. Bevformer: Learning bird's-eye-view representation from multi-camera images via spatiotemporal transformers. *arXiv preprint arXiv:2203.17270*, 2022. 5

[13] Bencheng Liao, Shaoyu Chen, Xinggang Wang, Tianheng Cheng, Qian Zhang, Wenyu Liu, and Chang Huang. Maptr: Structured modeling and learning for online vectorized hd map construction. *arXiv preprint arXiv:2208.14437*, 2022. 1

[14] Lingjie Liu, Jiatao Gu, Kyaw Zaw Lin, Tat-Seng Chua, and Christian Theobalt. Neural sparse voxel fields. In *NeurIPS*, 2020. 3

[15] Yicheng Liu, Yue Wang, Yilun Wang, and Hang Zhao. Vectormapnet: End-to-end vectorized hd map learning. *arXiv preprint arXiv:2206.08920*, 2022. 1, 5

[16] Ze Liu, Yutong Lin, Yue Cao, Han Hu, Yixuan Wei, Zheng Zhang, Stephen Lin, and Baining Guo. Swin transformer: Hierarchical vision transformer using shifted windows. In *Proceedings of the IEEE/CVF International Conference on Computer Vision*, pages 10012–10022, 2021. 4

[17] Chenyang Lu, Marinus Jacobus Gerardus van de Molengraft, and Gijs Dubbelman. Monocular semantic occupancy grid mapping with convolutional variational encoder–decoder networks. *IEEE Robotics and Automation Letters*, 4(2):445–452, 2019. 2

[18] Gellert Mattyus, Shenlong Wang, Sanja Fidler, and Raquel Urtasun. Enhancing road maps by parsing aerial images around the world. In *Proceedings of the IEEE international conference on computer vision*, pages 1689–1697, 2015. 2

[19] Gellért Máttyus, Shenlong Wang, Sanja Fidler, and Raquel Urtasun. Hd maps: Fine-grained road segmentation by parsing ground and aerial images. In *Proceedings of the IEEE Conference on Computer Vision and Pattern Recognition*, pages 3611–3619, 2016. 2

[20] Lars Mescheder, Michael Oechsle, Michael Niemeyer, Sebastian Nowozin, and Andreas Geiger. Occupancy networks: Learning 3d reconstruction in function space. In *CVPR*, 2019. 3

[21] Bowen Pan, Jiankai Sun, Ho Yin Tiga Leung, Alex Andonian, and Bolei Zhou. Cross-view semantic segmentation for sensing surroundings. *IEEE Robotics and Automation Letters*, 5(3):4867–4873, 2020. 3

[22] Jeong Joon Park, Peter Florence, Julian Straub, Richard Newcombe, and Steven Lovegrove. DeepSDF: Learning Continuous Signed Distance Functions for Shape Representation. In *CVPR*, 2019. 3

[23] Jonah Philion and Sanja Fidler. Lift, splat, shoot: Encoding images from arbitrary camera rigs by implicitly unprojecting to 3d. In *European Conference on Computer Vision*, pages 194–210. Springer, 2020. 3, 5

[24] François Pomerleau, Francis Colas, Roland Siegwart, et al. A review of point cloud registration algorithms for mobile robotics. *Foundations and Trends® in Robotics*, 4(1):1–104, 2015. 2

[25] Zequn Qin, Jingyu Chen, Chao Chen, Xiaozhi Chen, and Xi Li. Uniformer: Unified multi-view fusion transformer for spatial-temporal representation in bird's-eye-view. *arXiv preprint arXiv:2207.08536*, 2022. 7

[26] Thomas Roddick and Roberto Cipolla. Predicting semantic map representations from images using pyramid occupancy networks. In *Proceedings of the IEEE/CVF Conference on Computer Vision and Pattern Recognition*, pages 11138–11147, 2020. 3

[27] Guodong Rong, Byung Hyun Shin, Hadi Tabatabaee, Qiang Lu, Steve Lemke, Mārtiņš Možeiko, Eric Boise, Geehoon Uhm, Mark Gerow, Shalin Mehta, et al. Lgsvl simulator: A high fidelity simulator for autonomous driving. *arXiv preprint arXiv:2005.03778*, 2020. 2

[28] Avishkar Saha, Oscar Mendez, Chris Russell, and Richard Bowden. Translating images into maps. In *2022 International Conference on Robotics and Automation (ICRA)*, pages 9200–9206. IEEE, 2022. 3

[29] Shunsuke Saito, Zeng Huang, Ryota Natsume, Shigeo Morishima, Angjoo Kanazawa, and Hao Li. PIFu: Pixel-Aligned Implicit Function for High-Resolution Clothed Human Digitization. In *ICCV*, 2019. 3

[30] Aleksandr Segal, Dirk Haehnel, and Sebastian Thrun. Generalized-icp. In *Robotics: science and systems*, volume 2, page 435. Seattle, WA, 2009. 2

[31] Jiaming Sun, Yiming Xie, Linghao Chen, Xiaowei Zhou, and Hujun Bao. Neuralrecon: Real-time coherent 3d reconstruction from monocular video. In *Proceedings of the IEEE/CVF Conference on Computer Vision and Pattern Recognition*, pages 15598–15607, 2021. 3

[32] Shenlong Wang, Min Bai, Gellert Mattyus, Hang Chu, Wenjie Luo, Bin Yang, Justin Liang, Joel Cheverie, Sanja Fidler, and Raquel Urtasun. Torontocity: Seeing the world with a million eyes. *arXiv preprint arXiv:1612.00423*, 2016. 2

[33] Shenlong Wang, Sanja Fidler, and Raquel Urtasun. Holistic 3d scene understanding from a single geo-tagged image. In *Proceedings of the IEEE Conference on Computer Vision and Pattern Recognition*, pages 3964–3972, 2015. 2

[34] Yue Wang, Vitor Campagnolo Guizilini, Tianyuan Zhang, Yilun Wang, Hang Zhao, and Justin Solomon. Detr3d: 3d object detection from multi-view images via 3d-to-2d queries. In *Conference on Robot Learning*, pages 180–191. PMLR, 2022. 3

[35] Bin Yang, Ming Liang, and Raquel Urtasun. Hdnet: Exploiting hd maps for 3d object detection. In *Conference on Robot Learning*, pages 146–155. PMLR, 2018. 2

[36] Sheng Yang, Xiaoling Zhu, Xing Nian, Lu Feng, Xiaozhi Qu, and Teng Ma. A robust pose graph approach for city scale lidar mapping. In *2018 IEEE/RSJ International Conference on Intelligent Robots and Systems (IROS)*, pages 1175–1182. IEEE, 2018. 2

[37] Weixiang Yang, Qi Li, Wenxi Liu, Yuanlong Yu, Yuexin Ma, Shengfeng He, and Jia Pan. Projecting your view attentively: Monocular road scene layout estimation via cross-view transformation. In *Proceedings of the IEEE/CVF Conference on Computer Vision and Pattern Recognition*, pages 15536–15545, 2021. 2

[38] Lior Yariv, Yoni Kasten, Dror Moran, Meirav Galun, Matan Atzmon, Basri Ronen, and Yaron Lipman. Multiview neural surface reconstruction by disentangling geometry and appearance. In *NeurIPS*, 2020. 3

[39] Yurong You, Katie Z Luo, Xiangyu Chen, Junan Chen, Wei-Lun Chao, Wen Sun, Bharath Hariharan, Mark Campbell, and Kilian Q Weinberger. Hindsight is 20/20: Leveraging past traversals to aid 3d perception. *arXiv preprint arXiv:2203.11405*, 2022. 7

[40] Fisher Yu, Jianxiong Xiao, and Thomas Funkhouser. Semantic alignment of lidar data at city scale. In *Proceedings of the IEEE Conference on Computer Vision and Pattern Recognition*, pages 1722–1731, 2015. 2

[41] Brady Zhou and Philipp Krähenbühl. Cross-view transformers for real-time map-view semantic segmentation. *arXiv preprint arXiv:2205.02833*, 2022. 3